UNCLASSIFIED
(Approved for Publication)

CLM - P 38

# PERFORMANCE OF THE He - Ne GAS LASER AS AN INTERFEROMETER FOR MEASURING PLASMA DENSITY

by

D.E.T.F. ASHBY
D.F. JEPHCOTT
A. MALEIN
F.A. RAYNOR

## A B S T R A C T

The characteristics of the He - Ne gas laser used in a new simple interferometric technique have been studied experimentally and theoretically. The interferometer has two novel features; first, the intensity of the laser itself is used to detect the fringes and second, because the intensities of the 0.63 micron (red) and 3.39 micron (infra-red) laser beams are coupled, interference in the infra-red can be detected by a simple photomultiplier monitoring the red beam.

The system does not respond instantaneously to changes in the optical path length; experimental measurements show that when the red beam is used to follow interference in the infra-red the maximum detectable response is limited to about $3 \times 10^6$ fringes per second. Discussion of the frequency response and the cross-coupling between the two wavelengths leads to the conclusion that the frequency response is limited by the red channel only.

Experimental details of the interferometer are described, including the application of a multi-pass system which, with some loss in spatial resolution, increases the sensitivity of the interferometer by at least a factor of 20.

U.K.A.E.A. Research Group,
Culham Laboratory,
Nr. Abingdon,
Berks.

March, 1964

(C/18 IMG)

## CONTENTS


| | Page |
|---|---|
| INTRODUCTION | 1 |
| PRINCIPLES OF THE METHOD | 2 |
| Plasma Equations | 2 |
| Description of the Laser Interferometer | 3 |
| FREQUENCY RESPONSE AND CROSS-COUPLING | 4 |
| Experiments | 4 |
| Theory of Frequency Response | 5 |
| EXPERIMENTAL MEASUREMENT OF PLASMA DENSITY | 8 |
| PRACTICAL DETAILS | 10 |
| CONCLUSION | 13 |
| ACKNOWLEDGEMENTS | 14 |
| REFERENCES | 14 |

## 1. INTRODUCTION

This paper discusses the main aspects of a new interferometric technique which uses the 0.6328 micron (red) and 3.391 micron (infra-red) radiation from a He - Ne gas laser to measure the electron density in a plasma [1].

Interferometry using visible light is an established method of measuring plasma density [2,3], while the increased sensitivity associated with longer wavelengths has been exploited for many years in microwave interferometers [4]; in addition, an interferometer operating in the far infra-red has been developed recently [5]. The laser interferometer [6], however, has unique features which introduce major simplifications both in optical adjustment and in detection of the interference fringes. The interferometer uses only one mirror in addition to those in the laser, and the intensity of the laser itself is used to observe the fringes. Both laser wavelengths, i.e. 0.63 and 3.4 micron, are available for interferometry but interference in the infra-red can be detected by a photomultiplier tube measuring the intensity of the 0.63 micron radiation alone; no infra-red detector is necessary. The interferometer is suitable for measuring the density of plasmas which produce one or more fringes; with the infra-red radiation the condition for this is $\bar{n}_e \geqslant 3.3 \times 10^{16}/L \text{ cm}^{-3}$, where $\bar{n}_e$ is the average number density of electrons along the line of sight and $L$ is the length of the plasma in cm. Because the interferometer does not respond instantaneously to changes in optical path length, the system is not suitable for use with plasmas in which the electron density

changes very rapidly; a practical upper limit is about 3 fringes per microsecond.

## 2. PRINCIPLES OF THE METHOD

### Plasma Equations

The refractive index $\mu$ of a plasma for electromagnetic radiation of frequency $\omega/2\pi$, when $\omega$ is much greater than both the plasma frequency $\omega_p$ and the electron cyclotron frequency, is given by

$$\mu = 1 - \tfrac{1}{2}(\omega_p/\omega)^2 \qquad \ldots (1)$$

where

$$\omega_p^2 = 4\pi n_e e^2/m_e .$$

Thus the electron number density $n_e$ of a plasma can be found by measuring its refractive index with an interferometer using radiation of a suitable frequency. The number $N$ of interference fringes produced by a plasma of length $L$ is given by

$$N = (\mu - 1)2L/\lambda \qquad \ldots (2)$$

where $\lambda$ is the radiation wavelength and the interferometer beam has a total path length of $2L$ within the plasma.

From equations (1) and (2),

$$N = (\omega_p/\omega)^2 \, L/\lambda$$

$$= 8.9 \times 10^{-14} \, n_e \, L\lambda \, . \qquad \ldots (3)$$

Note that the number of fringes is proportional to the wavelength used.

## Description of the Laser Interferometer

When the output beam from a laser is reflected back into the optical cavity by means of an external mirror, the whole laser intensity is strongly influenced by any phase change in the reflected radiation. The laser intensity undergoes one cycle of modulation for each complete wavelength change in the optical path between the laser and the external mirror, thus the cycles of modulation correspond to the fringes of a conventional interferometer. This effect was observed by King and Steward [6] who showed that it enabled long path length interferometry to be carried out with a C.W. He - Ne gas laser and one external mirror. The He - Ne laser is particularly useful in this application because it can generate simultaneously both visible light at 0.63 micron wavelength and infra-red at 3.4 micron. The presence of the visible beam simplifies optical alignment, and both wavelengths are available for interferometry. Furthermore, because the two wavelengths arise from a common upper energy level ($3s_2$) in the neon atom [7] there is a coupling between the radiation intensities at the two wavelengths; any modulation in the intensity of laser action at 3.4 micron produces a complementary modulation in the intensity of the 0.63 micron radiation. Thus interference in the infra-red can be detected by an ordinary photomultiplier which responds only to visible light. We can therefore take advantage of the increased sensitivity associated with the longer wavelength (equation (3)) and at the same time retain the convenience of working with visible light.

The reciprocal effect, i.e. modulation of the infra-red intensity caused by interference in the red, is not observed so the coupling in this direction is assumed to be weak.

## 3. FREQUENCY RESPONSE AND CROSS-COUPLING

### Experiments

The maximum rate of change of optical path length which the interferometer can detect was measured by using a rotating mirror to reflect the output beam back into the laser. The beam was directed to one side of the axis of rotation so that at one instant in each revolution the beam was reflected by a portion of the mirror moving towards the laser. Modulation at the Doppler frequency corresponding to the mirror velocity was observed, the depth of modulation decreasing as the frequency increased. Figure 1 shows how the depth of modulation of the red output from the laser varies with frequency when interference takes place in first the infra-red and then the red; in both cases the modulation is expressed as a fraction of that observed with low frequency infra-red fringes. With interference in the infra-red the depth of modulation has fallen to 1/e at 150 kc/s and the upper frequency limit of detection is about 3 Mc/s. This limit implies that the maximum rate of change of $\bar{n}_e$ which can be measured when the red output is used to detect infra-red fringes is

$$\frac{d\bar{n}_e}{dt} \approx 10^{23}/L \text{ cm}^{-3} \text{ sec}^{-1} .$$

The upper limit here is imposed not by the detector but by the response of the laser itself. If, on the other hand, the infra-red output is used to detect infra-red fringes then the upper frequency limit

($\approx$ 100 kc/s) is determined by the time response of commercially available detectors.

The complementarity of modulation in the red and infra-red radiation is shown in Figure 2. These oscillograms were obtained when interference occurred in the infra-red radiation as a result of random vibrations of the external mirror which reflected the beam back into one end of the laser. The intensity of the red beam from the other end of the laser was measured by a photomultiplier and at the same time the infra-red intensity was measured by an indium antimonide detector; both beams were interrupted at 800 c/s by a rotating slotted disc so that the depth of modulation of each could be seen. The upper trace is the output from the photomultiplier (signal increasing downwards) and the lower trace is that from the infra-red detector (signal increasing upwards). By adjusting the gains of the oscilloscope amplifiers the two traces can be made to match like two pieces of a jig-saw puzzle, showing the high degree of complementarity between the intensities of the two beams.

## Theory of Frequency Response

The variation in the intensities $\varepsilon_1$ and $\varepsilon_2$ of radiation at the two wavelengths can be represented by the pair of coupled non-linear differential equations

$$d\varepsilon_1/dt = a_1\varepsilon_1 + b_1\varepsilon_1^2 + c_1\varepsilon_1\varepsilon_2 \qquad \ldots (4)$$

$$d\varepsilon_2/dt = a_2\varepsilon_2 + b_2\varepsilon_2^2 + c_2\varepsilon_1\varepsilon_2 \qquad \ldots (5)$$

where the 'a' terms represent the combined effect of stimulated emission, absorption and mirror losses, the 'b' terms represent the reduction in the population inversion as the radiation intensity increases, and the 'c' terms take account of the cross-coupling, i.e. the depopulation of the

upper level by laser action at the other wavelength. For laser action to occur it is necessary that $a > 0$. The equilibrium intensities are given by

$$\varepsilon_{1o} = (a_2c_1 - a_1b_2)/(b_1b_2 - c_1c_2) \qquad \ldots (6)$$

$$\varepsilon_{2o} = (a_1c_2 - a_2b_1)/(b_1b_2 - c_1c_2) \qquad \ldots (7)$$

If now interference occurs in the red light (subscript 1, say) and the optical path is changing such that fringes appear at the frequency $\omega/2\pi$ then the intensity modulation in the red, $\tilde{\varepsilon}_1$, is obtained by assuming $a_1$ to have a small oscillating part $\tilde{a}_1 e^{i\omega t}$ and carrying out a linearised perturbation analysis to give

$$\tilde{\varepsilon}_1 \left[ (i\omega - b_1\varepsilon_{1o}) - \frac{c_1c_2\varepsilon_{1o}\varepsilon_{2o}}{(i\omega - b_2\varepsilon_{2o})} \right] = \tilde{a}_1\, \varepsilon_{1o} \qquad \ldots (8)$$

If interference occurs in the infra-red (subscript 2) and the intensity of the red light is measured then we have

$$\tilde{\varepsilon}_1 \left[ (i\omega - b_1\varepsilon_{1o}) - \frac{c_1c_2\varepsilon_{1o}\varepsilon_{2o}}{(i\omega - b_2\varepsilon_{2o})} \right] = \frac{\tilde{a}_2c_1\varepsilon_{1o}\varepsilon_{2o}}{(i\omega - b_2\varepsilon_{2o})} \qquad \ldots (9)$$

Since the observed frequency responses in the two cases are the same we conclude that over the experimental range

$$\omega \ll b_2\varepsilon_{2o} \qquad \ldots (10)$$

which leads to a common frequency response given by the simple relation

$$(\tilde{\varepsilon})_\omega / (\tilde{\varepsilon})_{\omega=o} = \left(1 + \frac{i\omega}{\omega_o}\right)^{-1} \qquad \ldots (11)$$

$$\text{i.e.} \quad \left|(\tilde{\varepsilon})_\omega\right| \Big/ \left|(\tilde{\varepsilon})_{\omega=o}\right| = \left[ 1 + \left(\frac{\omega}{\omega_o}\right)^2 \right]^{-\frac{1}{2}} \qquad \ldots (12)$$

where

$$\omega_o = (a_1b_2 - a_2c_1)/b_2 \ .$$

A good fit is obtained to both sets of experimental points in Figure 1 with $\omega_0/2\pi = 45$ kc/s.

If we apply the condition $\omega \ll \omega_0$ and calculate the fractional depths of modulation $P_1$ and $P_2$ of the red and infra-red intensities when interference is taking place in the infra-red we obtain

$$(P_1/P_2)_{i.r.} = c_1\varepsilon_{20}/b_1\varepsilon_{10} \ . \qquad \ldots (13)$$

For the other case, when interference occurs in the red,

$$(P_1/P_2)_{r} = b_2\varepsilon_{20}/c_2\varepsilon_{10} \ . \qquad \ldots (14)$$

Experimentally, the first ratio was approximately unity and the second ratio much greater than one, so we have

$$c_1\varepsilon_{20}/b_1\varepsilon_{10} \approx 1 \ , \qquad \ldots (15)$$

$$b_2\varepsilon_{20}/c_2\varepsilon_{10} \gg 1 \ . \qquad \ldots (16)$$

Referring to the original equations (4) and (5) these inequalities simply mean that the cross-coupling term is relatively unimportant as far as the infra-red intensity is concerned while for the red it is of comparable importance with the direct non-linear term.

If interference in the infra-red is detected in the infra-red we have

$$\tilde{\varepsilon}_2 \left[ (i\omega - b_2\varepsilon_{20}) - \frac{c_1c_2\varepsilon_{10}\,\varepsilon_{20}}{(i\omega - b_1\varepsilon_{10})} \right] = \tilde{a}_2\varepsilon_{20} \ . \qquad \ldots (17)$$

Applying the conditions (10), (15) and (16) to equation (17) we obtain

$$(\tilde{\varepsilon}_2)_{\omega} / (\tilde{\varepsilon}_2)_{\omega = 0} \approx 1 \ .$$

The overall conclusion is that the frequency response of the interferometer is at present limited by the red light channel only; a substantial increase in the maximum observable fringe rate could be expected if a fast infra-red detector were available to measure the modulation of the infra-red beam directly.

Note also that, because equation (8) is complex, some distortion due to phase shift may be expected when the band width of the fringe signal includes the critical frequency $\omega_0$. This may introduce a maximum error of ¼ of a fringe into the simple fringe counting technique.

## 4. EXPERIMENTAL MEASUREMENT OF PLASMA DENSITY

The laser interferometer has been used to measure the electron density in a pulsed gas discharge; a short account of this work has already been given[1]. Figure 3 is a diagram of the experiment. The discharge tube is in the optical path between the laser and the external mirror and as the electron density changes during the discharge pulse the laser intensity goes through successive maxima and minima which correspond to interference fringes. The laser intensity is highly sensitive to the presence of the reflected beam; 1% of the output beam intensity reflected back to the laser is sufficient to modulate the whole intensity by 50%. The lower traces in Figures 4a and 4b are infra-red fringes detected by a photomultiplier which measured the red light intensity, while the upper traces show the gas discharge current; oscillograms 4a and 4b have different sweep speeds. The electron density at any time in the discharge is determined simply by counting fringes and using equation (3); in Figure 4a the time of maximum electron density

is shown by the 'saddle' in the fringe pattern. Figure 5 shows red fringes obtained on the same discharge when the infra-red beam was suppressed by a plain glass filter. The ratio of the number of infra-red to the number of red fringes agrees with the ratio of the two wavelengths to within the experimental error.

There is no difficulty in counting the fringes in Figures 4 and 5 because the electron density changes in a regular manner. In plasmas where large irregular fluctuations in density occur the fringe pattern may not be readily interpretable and care is needed in counting the fringes; in these cases comparison of measurements at the two wavelengths may provide a useful check.

The non-linear relation between the laser intensity and the phase of the reflected radiation is shown by the pointed character of the fringes in Figure 4. Fringes more sinusoidal in shape can be obtained by reducing the intensity of the reflected radiation; on the other hand if the intensity of the reflected beam is increased the fringes eventually develop flat bottoms when destructive interference completely stops the infra-red laser action. The non-sinusoidal shape of the fringes makes the interferometer unsuitable for use with plasmas which produce less than one fringe.

In the arrangement of Figure 3 the laser beam is divergent and the area of the reflected beam at the laser is about 100 times that of the output beam, thus only a small fraction of the output energy is injected back into the laser. Because of the beam divergence, the additional optical cavity formed by the external mirror can be regarded as having

a low Q value. A modification of the system has been reported[8], in which the additional cavity has a high Q giving increased sensitivity.

## 5. PRACTICAL DETAILS

The laser used in this work (see Figure 6) was made at S.E.R.L., Baldock. The quartz discharge tube, 0.7 cm bore and 70 cm long, contains 86% helium and 14% neon at a pressure of 1.2 Torr. An R.F. discharge is excited by a 36 Mc/s oscillator which can supply about 80 watts to the discharge tube. The optical cavity is formed by two mirrors, one plane and one concave (150 cm focal length) mounted at the ends of an aluminium tube 80 cm long. Each mirror has a multi-layer dielectric coating designed to give a reflectivity of about 0.98 at 0.63 micron wavelength. The coatings were not designed to produce any particular reflectivity at 3.4 micron and measurements made on batches of laser mirrors show that reflectivities at 3.4 micron may vary between 0.02 and 0.2, depending on the manufacturer and the number of layers. In general, mirrors with 15 layer coatings are found to have a reflectivity of 0.15 to 0.2 at 3.4 micron, which is sufficient to produce laser action at this wavelength, providing the R.F. power input to the discharge tube is about 80 watts; if the power input is reduced much below this level, only the red output remains.

The effect of diffraction plus that of the concave mirror in the laser is to produce a beam which is slightly divergent. The diameter of the red beam increases from about 0.15 cm close to the laser to 0.8 cm over a distance of 500 cm; the divergence of the infra-red is about twice that of the red. Only the portion of the return beam which is

superimposed on the output beam contributes to the interference; this can be demonstrated by reducing the diameter of the return beam to that of the outgoing beam by means of a stop. Hence the beam divergence does not decrease spatial resolution in the plane perpendicular to the beam direction. Because the depth of modulation depends on the intensity of the return beam the modulation can be increased by converging the beam with an external concave mirror in place of the normal plane mirror.

With one double pass, i.e. with the laser beam traversing a total path length of $2L$ in the plasma, the number of infra-red fringes is

$$N = \bar{n}_e L/3.3 \times 10^{16} .$$

This sensitivity can be increased by using a multi-pass system; a convenient arrangement is that suggested by White[9] for use in molecular absorption spectroscopy. Figure 7a shows the essential features of the system with four double passes. Three concave mirrors A B and C of the same radius of curvature are mounted as shown with mirror B at a distance from A and C equal to the common radius of curvature. The laser beam passes through the system and is returned along its path by a fourth concave mirror D; the beam is refocused on each reflection and its diameter remains less than 3 mm throughout its path. The number of passes is increased by tilting the mirrors A and C; Figure 7b shows the ray diagram for 8 double passes. The interferometer has been operated satisfactorily at 3.4 micron with 20 double passes between mirrors of 200 cm radius of curvature. In any particular application the number of useful passes may be limited by reflection losses at the mirror surfaces, by absorption losses in intervening windows or

by spurious fringes produced by vibration of the mirrors. In an ordinary laboratory with no special precautions taken to isolate the optical components from floor or air-borne vibrations, spurious infra-red fringes occurred at a maximum rate of roughly 100 n per second, where n is the number of double passes. A further limitation to the number of passes is imposed by the unavoidable decrease in spatial resolution as the number of passes increases; for example, the cross-sectional area sampled by the beam increased from a circle of 0.3 cm diameter with one double pass to a rectangle 2 cm × 0.5 cm with the 20 double passes mentioned above.

To detect fringes occurring at frequencies up to about 500 kc/s, almost any photomultiplier tube can be used; a stop of the same diameter as the laser beam and a red filter (Wratten 25) are necessary to reduce background light from the R.F. discharge in the laser tube. As the frequency of the fringes increases their amplitude decreases (see Figure 5) and the upper frequency limit of detection is determined by the noise level of the photomultiplier. Different P.M. tubes were tried; the best signal to noise ratio was obtained with an E.M.I. 9637 TA which is a 'venetian blind' tube with a tri-alkali photocathode and 5 dynodes.

In some applications trouble may arise from unwanted photomultiplier signals caused by background light from the plasma itself; this can be reduced simply by moving the laser and photomultiplier further away from the plasma. The interferometer operates satisfactorily over lengths of 20 metres or more and there is no particular virtue in working close to the experimental plasma; indeed, this should be avoided if large stray magnetic fields are present because they may cause unwanted movement of

the optical components and complicate the laser operation by the Zeeman splitting of energy levels.

## 6. CONCLUSION

Among the generally accepted techniques for measuring electron density in plasmas, interferometry has the advantage of providing readily interpretable experimental data, independent of the electron temperature. In spite of this advantage only microwave interferometers have been widely used in experimental plasma physics and these are limited to low density plasmas ($n_e < 10^{14}$ cm$^{-3}$) by the frequency of available microwave generators ($< 1.5 \times 10^{11}$ c/s). Optical interferometers, which are capable of examining much denser plasmas, have had limited use as practical diagnostic instruments. This is partly because plasmas of current interest are not sufficiently refractive to visible light and partly because of the difficulty of setting up and adjusting the components of a conventional interferometer around the complex and inaccessible apparatus commonly encountered in modern plasma physics.

The interferometer which has been described largely overcomes both of these difficulties. The use of infra-red radiation, together with the ease of using a multi-pass system, readily increases the number of fringes and makes possible interferometry on plasmas which are not strongly refractive to visible light. But the main advantage of the system is its simplicity; the laser itself acts as both light source and fringe shift detector and the only optical adjustment required is the alignment of a single mirror.

ACKNOWLEDGEMENTS

The authors wish to thank the laser group at S.E.R.L., Baldock, under Dr. H.A.H. Boot, for their ready co-operation and for the loan of equipment used in this work. Particular thanks are due to P.G.R. King and N.H. Rock of S.E.R.L. for useful discussions, and to Dr. R.J. Bickerton of the Culham Laboratory for his theoretical treatment.

REFERENCES

1. ASHBY, D.E.T.F. and JEPHCOTT, D.F., App. Phys. Lett., 3, 13 (1963)

2. ALPHER, R.A. and WHITE, D.R., Phys. Fluids, 2, 162 (1959)

3. DYSON, J., WILLIAMS, R.V. and YOUNG, K.M., Nature, 195, 1291 (1962)

4. WHITMER, R.F., Phys. Rev. 104, 572 (1956)

5. BROWN, S.C., 4th Annual Meeting, Division of Plasma Physics, American Physical Society, Atlantic City. November, 1962.

6. KING, P.G.R., and STEWARD, G.J., New Scientist, 17, 180 (1963)

7. BLOOM, A.L., BELL, W.E. and REMPEL, R.E., Appl. Opt., 2, 317, (1963).

8. GERARDO, J.B. and VERDEYEN, J.T., Appl. Phys. Lett., 3, 121, (1963).

9. WHITE, J.U., J. Opt. Soc. Amer., 32, 285, (1942).

## FIGURE CAPTIONS

Fig. 1 Depth of modulation of red output against frequency, for interference in the red and infra-red.

Fig. 2 Complementarity of the red and infra-red radiation.
Upper trace, 0.63 micron intensity
Lower trace, 3.4 micron intensity.

Fig. 3 Diagram of the interferometer measuring electron density in a gas discharge.

Fig. 4a Upper trace, discharge current. Lower trace, infra-red fringes. Sweep speed, 50 μsec per large division.

Fig. 4b Upper trace, discharge current. Lower trace, infra-red fringes. Sweep speed, 500 μsec per large division.

Fig. 5a Red Fringes. Sweep speed, 50 μsec per large division.

Fig. 5b Red Fringes. Sweep speed, 500 μsec per large division.

Fig. 6 The laser.

Fig. 7a Optical arrangement for 4 double passes.

Fig. 7b Optical arrangement for 8 double passes.

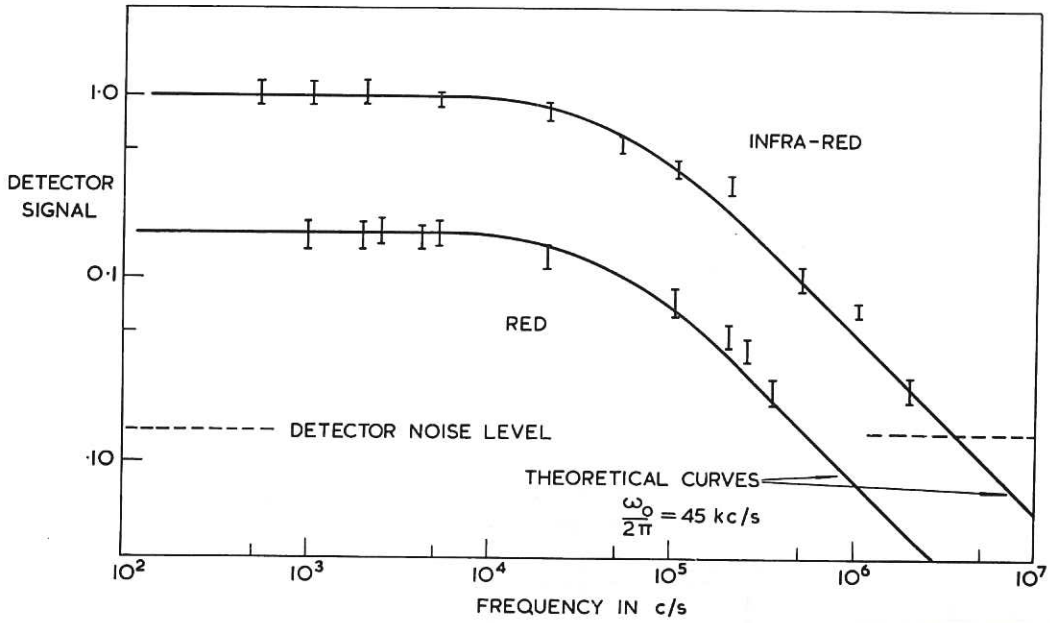


CLM-P 38 Fig. 1
Depth of modulation of red output against frequency, for interference in the red and infra-red.

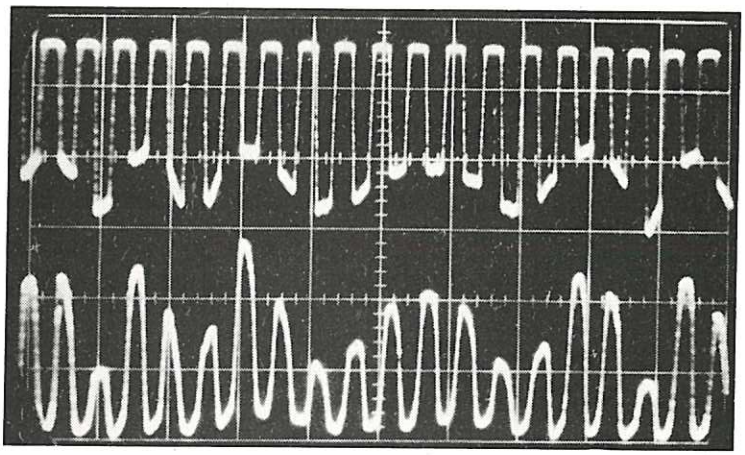

CLM-P 38 Fig. 2
Complementarity of the red and infra-red radiation.
Upper trace, 0.63 micron intensity.
Lower trace, 3.4 micron intensity.

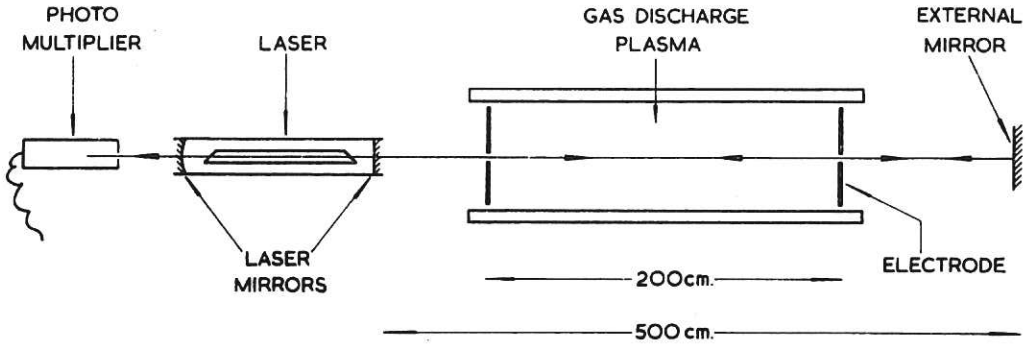


CLM - P 38 Fig. 3

Diagram of the interferometer measuring electron density in a gas discharge.

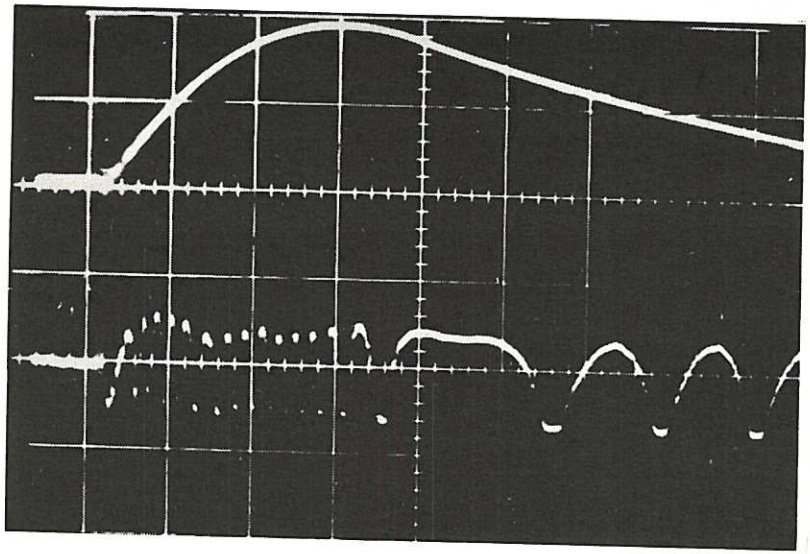

CLM-P 38 Fig. 4a
Upper trace, discharge current. Lower trace, infra-red fringes.
Sweep speed, 50 $\mu$sec per large division.

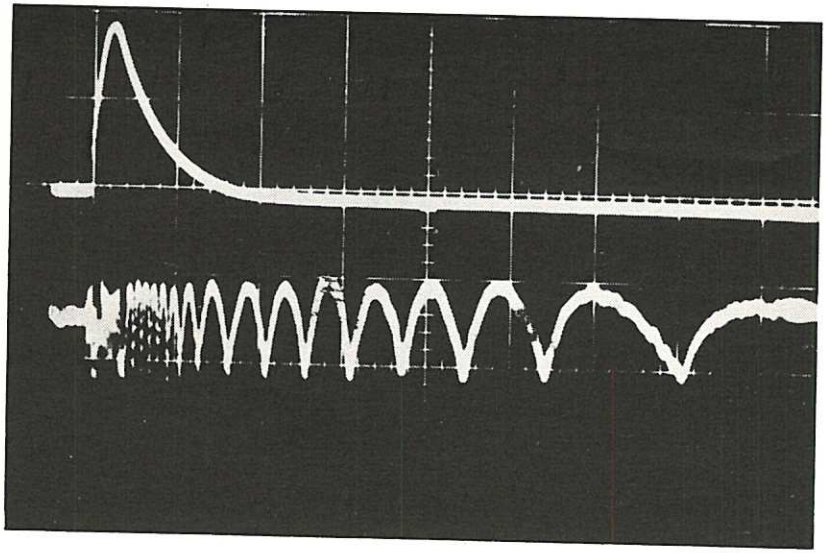

CLM-P 38 Fig. 4b
Upper trace, discharge current. Lower trace, infra-red fringes.
Sweep speed, 500 $\mu$sec per large division.

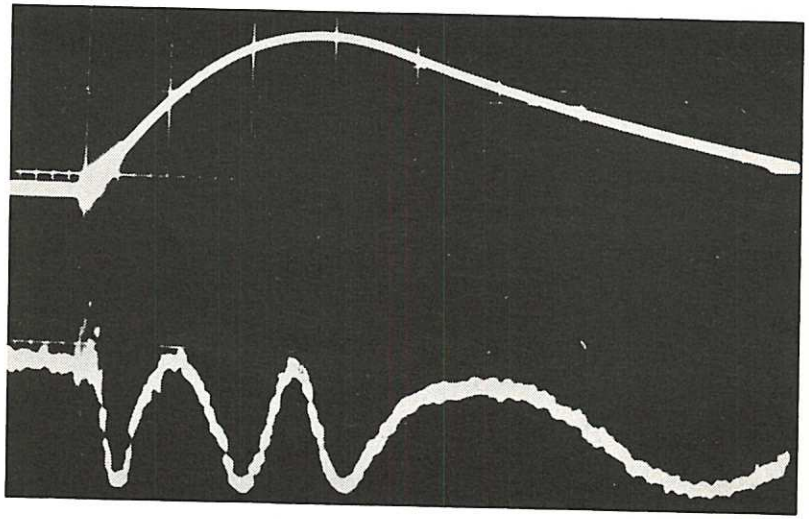

CLM-P 38 Fig. 5a
Red fringes. Sweep speed, 50 $\mu$sec per large division.

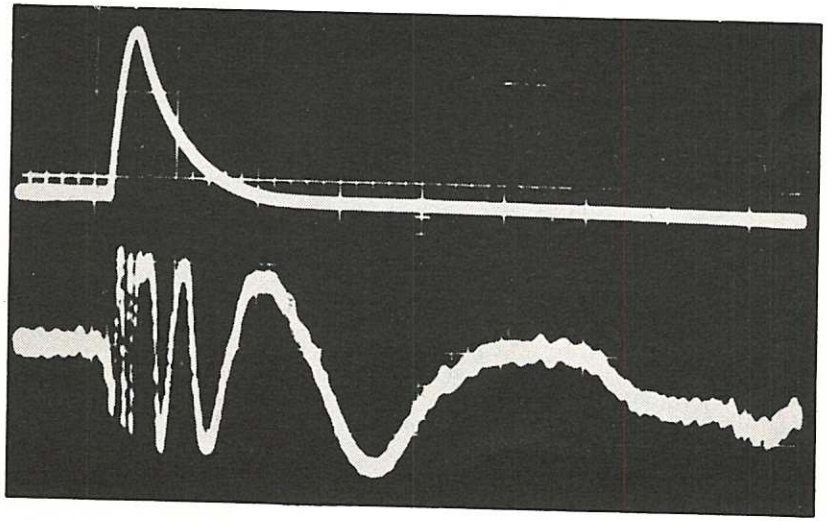

CLM-P 38 Fig. 5b
Red fringes. Sweep speed, 500 $\mu$sec per large division.

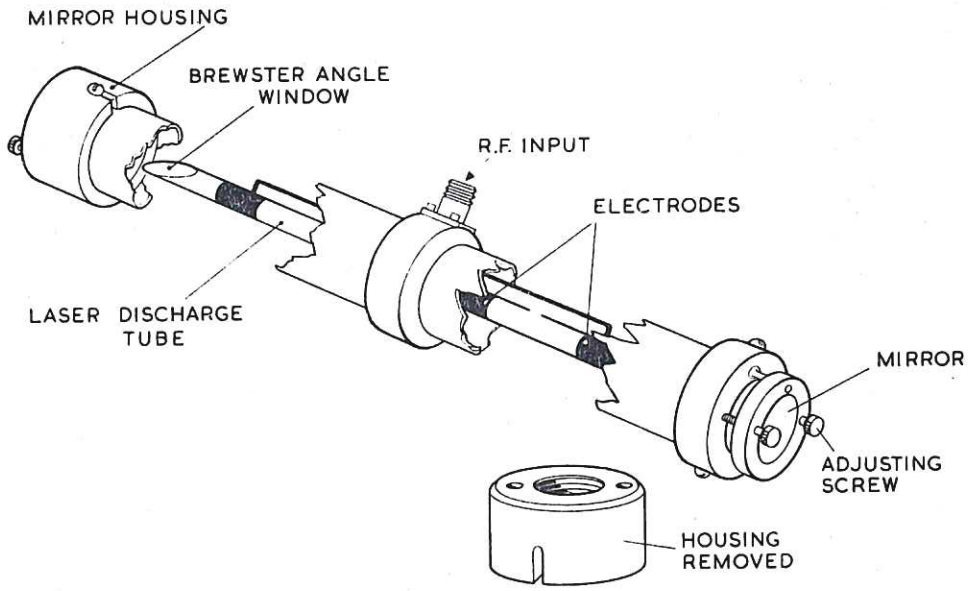


CLM-P 38 Fig. 6 The laser.

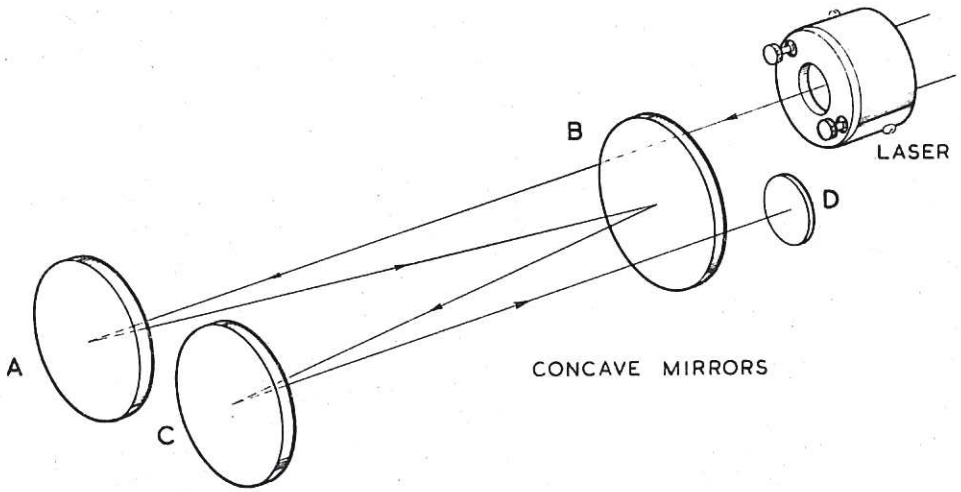


CLM-P 38 Fig. 7a
Optical arrangement for 4 double passes.

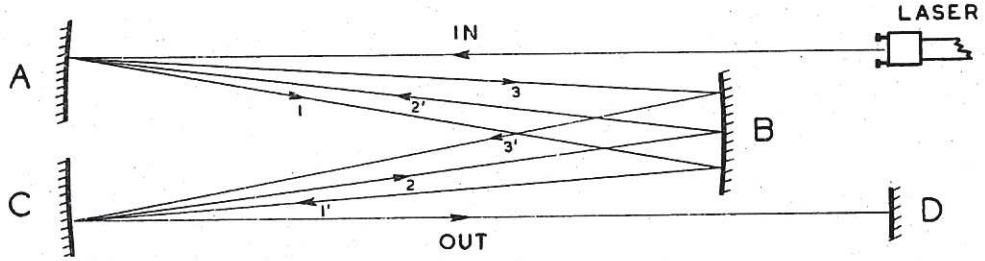


CLM-P 38 Fig. 7b
Optical arrangement for 8 double passes.